A Numerical Model for Charge Transport and Recombination in Dye-Sensitized Solar Cells

Juan A. Anta,*,† Fabiola Casanueva,† and Gerko Oskam‡

Área de Química Física, Universidad Pablo de Olavide, Sevilla, Spain, and Departamento de Física Aplicada, CINVESTAV−IPN, Mérida, Yucatán, México

Received: November 9, 2005; In Final Form: January 27, 2006

We propose a numerical model aimed at obtaining the electrical output of dye-sensitized solar cells from microscopic parameters. The model is based on the solution of the continuity equation as a function of voltage for electron transport with both the diffusion coefficient and the recombination constant dependent on the electron density, i.e., the light intensity and/or voltage. The density dependence of the kinetic parameters can be implemented in analytical form (via a power-law expression) or extracted from experiments or electron transport simulations. We investigate the situation where the recombination rate is limited by the electron transport in the nanostructured film, as has recently been suggested by various authors. It is observed that for a power-law density dependence governed by a single α parameter, related to the depth and shape of a trap energy distribution, the solar cell behaves as an ideal diode, where the short-circuit current, open-circuit voltage, and current−voltage characteristics are independent of the α parameter. According to the formal description provided here, where recombination is limited by electron transport, lowering the trap density or changing α by changing the morphology or materials properties, thus improving the conductivity, would not lead to a better performance of the solar cell under steady-state conditions. The numerical results are compared to intensity-dependent current−voltage measurements on chlorophyll-sensitized TiO_2 solar cells.

Introduction

Solar cells based on sensitized nanostructured, mesoporous metal oxides (dye-sensitized solar cells, DSSCs) have attracted considerable attention since the work of O'Regan and Grätzel in 1991.[1] These devices are promising in the field of photovoltaics because they yield a good photoconversion efficiency, currently of 11%,[2] and have potentially lower fabrication costs than conventional silicon-based solar cells, due to the low costs of materials and the simplicity of the fabrication process. Further optimization of the DSSC requires a better insight into the interrelated processes of transport and accumulation of electrons in the mesoporous oxide phase and recombination of electrons with electron acceptors.[3−5]

In DSSCs photocurrents and photovoltages arise from a subtle balance of transport of photogenerated electrons toward the external circuit and recombination of these electrons with acceptors present in the system. In this context, it is commonly accepted that transport of electrons through the nanostructured network occurs mainly by diffusion.[6,7] This is due to the small size of the nanoparticles, which are unable to sustain a significant electrical field in the presence of a highly concentrated electrolyte solution.[3,8] Furthermore it is generally observed that diffusion of electrons in nanostructured films such as TiO_2 and ZnO is very slow, which is generally ascribed to trapping of electrons in surface defects.[9−12] With increasing electron density, the quasi-Fermi energy of the electrons shifts closer to the conduction band edge, such that the trap depth involved in the electron transport process decreases with increasing light intensity. Hence, due to the trap-filling effect,[13,14] the diffusion coefficient is found to increase with light intensity.[16] The influence of trapping on the diffusion coefficient leads to a special case of transport known as "dispersive transport" or "anomalous diffusion".[15] Anomalous diffusion has been introduced in the modeling of DSSCs by means of continuous time random walk (CTRW) simulations[5,13,14] or by solving the diffusion (continuity) equation for a density-dependent diffusion coefficient.[16]

Recombination of photogenerated electrons is the other main kinetic process that determines the photocurrent and photovoltage in DSSCs. Recombination is important because it limits the collection efficiency of electrons in the external circuit, especially when the cell is in series with an external resistive load. The kinetics of recombination are characterized by the electron lifetime, which has also been observed to depend strongly on light intensity.[17,18] This dependence has been attributed to the influence that anomalous diffusion itself has on the kinetics of recombination.[18,19] In other words, recombination of electrons appears to be limited by diffusion and trapping of electrons. Therefore, the corresponding kinetic constant should be also density-dependent.

In this work we implement a transport model that takes these features into account. The model proposed here is based on the numerical solution of the continuity equation with density-dependent diffusion and recombination constants. The actual mathematical form of this density dependence is an important issue, and experiments,[17,19] CTRW simulations,[14] and theoretical considerations[20] show that this dependence takes a power-law form, with the exponent related to the average depth of an exponential distribution of trap energies. The need for this macroscopic model becomes specially evident if we take into account that the implementation of random walk simulations of the complete nanostructured electrode (that is, assuming macroscopic dimensions resulting from the distance between

* Author to whom correspondence should be addressed. E-mail: jaantmon@upo.es.
† Universidad Pablo de Olavide.
‡ CINVESTAV−IPN.

10.1021/jp056493h CCC: $33.50
Published on Web 03/04/2006

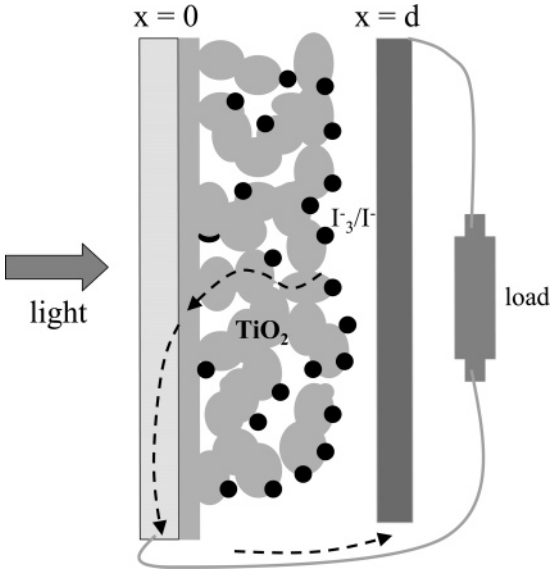

Figure 1. Schematic illustration of a dye-sensitized solar cell. The dashed arrow represents the electron current that is considered in the model. Gray and black circles stand for the TiO_2 nanoparticles and the adsorbed dye molecules, respectively.

the collecting and the counter electrode) is computationally very expensive.[7] The model presented in this work is aimed to be used in combination with simulations of electron transport in a small, microscopic part of the system in which the electron density is assumed to be constant.[14] Additionally, any other procedure, either experimental or theoretical, which is able to elucidate the electron density dependence of the diffusion coefficient and recombination constant, can be used as input to this model. In this paper we pay special attention to the evaluation of the current−voltage curve and the prediction of the open-circuit photovoltage as a function of the light intensity.

Electron Transport Model in DSSCs

Macroscopic Model: Continuity Equation for Electrons. Within the macroscopic model considered in this work, we evaluate the diffusion of electrons[21] through the nanostructured oxide film with variable generation and recombination terms and with appropriate boundary conditions. Electrons are injected into the system as a consequence of illumination through the back contact (Figure 1), and this implies that generation is a function of position. Electrons are allowed to diffuse toward the back contact (working electrode), which behaves as a collecting interface. Diffusion is governed by a density-dependent diffusion coefficient, and this means that this coefficient is also a function of position. In addition, electrons can "recombine" and disappear from the system. The kinetic constant that controls recombination has been found to depend on electron density; hence, it is also a function of the position. Finally the continuity equation is solved in a linear geometry; i.e., only the x-coordinate is considered (Figure 1). In summary, we solve numerically the following differential equation

$$\frac{\partial \rho(x,t)}{\partial t} = D_0 f(\rho) \frac{\partial^2 \rho(x,t)}{\partial^2 x} + D_0 \frac{\partial f(\rho)}{\partial \rho}\left(\frac{\partial \rho(x,t)}{\partial x}\right)^2 + G(x) - k_{R,0} f(\rho)[\rho(x,t) - \rho_0] \quad (1)$$

where $\rho(x,t)$ is the number density of electrons (as a function of the distance to the working electrode and time), D_0 and $k_{R,0}$ are the diffusion and recombination constants in the dark, and ρ_0 is the electron density in the dark. $G(x)$ is the generation term, which represents the number of electrons that enter the system per unit volume and unit time. This is evaluated via the equation

$$G(x) = \phi_{inj} \int_{\lambda_{min}}^{\lambda_{max}} I_o(\lambda)\alpha_{ab}(\lambda) \exp[-\alpha_{ab}(\lambda)x]\, d\lambda \quad (2)$$

where α_{ab} is the absorption coefficient of the cell as a function of the wavelength λ, ϕ_{inj} is the quantum yield of injection, and $I(\lambda)$ is the incident photon flux. This is given by

$$I(\lambda) = \frac{2Fc}{\lambda^4}\left[\frac{1}{\exp(hc/\lambda kT)}\right] \quad (3)$$

where c is the speed of light, h is the Planck's constant, k is the Boltzmann constant, and T is the temperature. F is adjusted to give the required total irradiance (from 0.1 to 1 sun, with 1 sun being 100 mW/cm^2) at $T = 5960$ K.[27] Finally, the function $f(\rho)$ in eq 1 contains the density dependence of the diffusion coefficient and the recombination constant.

Equation 1 is solved by means of the forward time central space (FTCS) method using the Lax scheme.[22] The following boundary conditions are applied

$$\rho(x = 0, t) = \rho_o(V) \quad \rho(x, t = 0) = \rho_o(V) \quad \left.\frac{\partial \rho(x, t)}{\partial x}\right|_{x=d} = 0 \quad (4)$$

where V is the voltage and d the film thickness. Note that the electron density in the dark and in the working electrode ($x = 0$) is made to depend on the voltage. The actual form that this dependence takes will be discussed below. These boundary conditions assume that the electron density in the working electrode is essentially the same as its value in the dark, which is a consequence of fast electron transfer at the transparent conducting oxide (TCO)/mesoporous oxide interface.[23]

In summary, the input data to the model are: the thickness of the film, the absorption spectrum of the sensitizing dye (adsorbed onto the oxide surface), the irradiance with respect to 1 sun, the diffusion coefficient, recombination constant, and electron density in the dark as a function of voltage, the quantum yield of injection, and the actual form of the function $f(\rho)$, which contains the density-dependent effects. If $f(\rho)$ is taken to be a constant in eq 1, then we recover the ordinary diffusion equation (with generation and recombination terms). The main output parameter is the current density, which is computed from the density gradient at $x = 0$. If the diffusion coefficient depends strongly on electron density, then the calculation of the current can be numerically inaccurate. Nevertheless, we find that numerical errors can be minimized if we use

$$J(x = 0, t) = D_{1/2} \frac{\rho(x = \Delta x, t) - \rho(x = 0, t)}{\Delta x} \quad (5)$$

with

$$D_{1/2} = \frac{1}{2} D_0 [f(x = \Delta x, t) - f(x = 0, t)] \quad (6)$$

From the current we can obtain the incident photon-to-electron conversion efficiency (IPCE) using

$$\Phi(\text{IPCE}) = \frac{J(\text{electron m}^{-2}\,\text{s}^{-1})}{I(\text{photon m}^{-2}\,\text{s}^{-1})} \quad (7)$$

TABLE 1: Rise Times ($t_{1/2}$) and Currents for Chlorophyll DSSCs with No Recombination[a]

α	$t_{1/2}$ (s)	J_{sc} (mA cm^{-2})	ECCE
0.23	0.23	0.251	0.988
0.33	0.53	0.251	0.988
0.50	1.89	0.252	0.988

[a] The excitation irradiance was 1 sun according to eq 3.

and the external current collection efficiency (ECCE) using

$$\mathrm{ECCE} = \frac{J(\text{electron m}^{-2}\,\text{s}^{-1})}{I \times \mathrm{LHE} \times \phi_{\mathrm{inj}}\,(\text{injected electron m}^{-2}\,\text{s}^{-1})} \tag{8}$$

where LHE is the light-harvesting efficiency.

The continuity equation was solved using between 50 and 120 points in x-space and 10^5-10^6 time steps (depending on the time required to reach the stationary state). To check the accuracy of the numerical procedure we have performed calculations with $k_{R,0} = 0$, for which the ECCE ideally should be 1 (Table 1). We see that the numerical parameters mentioned above permit to obtain the current, IPCE, and ECCE with a maximum error of around 1%.

Microscopic Model: Density Dependence of Diffusion and Recombination Constants. As mentioned in the Introduction, it is well-known that electron diffusion coefficients and recombination constants in mesoporous oxide films depend strongly on light intensity and, consequently, on electron density. In previous work[14] we found that the steady-state mobility of electrons allowed to move in a network of traps is given by

$$\mu = \mu_c(\rho/N_t)^{(1-\alpha)/\alpha} \tag{9}$$

where μ_c is the electron mobility in the conduction band, N_t is the total density of traps, and α is the characteristic parameter of an exponential distribution of trap energies defined by

$$g(E) = \frac{\alpha N_t}{kT}\exp\left(\frac{\alpha E}{kT}\right) \tag{10}$$

where E is the energy of the trap with respect to the conduction band (defined positive) and α is a parameter that reflects the "sharpness" or "depth" of the distribution of trap states below the conduction band.[13] Thus, a smaller α implies that the distribution is deeper on average with respect to the conduction band and that the relative proportion of deep traps is larger.

Taking into account Einstein's relation, which establishes the proportionality between the mobility and the diffusion coefficient, we can write

$$D = D_0\, f(\rho) \tag{11}$$

with

$$f(\rho) = \left(\frac{\rho}{\rho_0}\right)^{(1-\alpha)/\alpha} \tag{12}$$

where D_0 is the diffusion coefficient at a certain reference density ρ_0 (which we assume to be the density in the dark, although formally any other "reference" can be assumed within the present model). Equation 12 implies a certain density dependence that should be used in the formulation of the continuity eq 1. For instance, if $\alpha = 0.5$ and $k_{R,0} = 0$, then we recover the case studied by Cao et al.[16] The same density dependence implicit to eq 12 has been derived from theoretical considerations by Bisquert and Vikhrenko[20] and from random walk simulations by Van de Lagemaat and Frank.[7]

As mentioned in the Introduction, in this model we assume that recombination is diffusion-limited and that eq 12 also applies to recombination.[19] Hence, we write

$$k_R = k_{R,0}\, f(\rho) \tag{13}$$

The power-law functionality contained in eqs 11−13 is in accordance with experiments using transient spectroscopies[18] and electrochemical techniques,[17] which have shown that the diffusion coefficient and the electron lifetimes vary with light intensity according to a power-law expression.[17,18,24] In this regard, it should be pointed out that the lifetime of electrons has been reported[18] to decay according to $\tau_{50\%} \propto \rho^{-1/\alpha}$, with $\alpha = 0.25-0.5$. Whether this α parameter corresponds to the trap depth parameter in eq 10 is a confusing point in the literature. However, theoretical derivations starting from an exponential distribution of trap energies show that both the diffusion coefficient and the recombination constant should vary with density according to eq 12. This also agrees with the fact that k_R should be proportional to the diffusion coefficient in a true diffusion-limited chemical reaction.

It has been pointed out[4,14] that there is no need for the use of an exponential function to describe the energy distribution of the intraband localized states. However, it has been shown that more realistic trap energy distributions also lead to a power-law dependence.[14] Despite this prevalence of the power-law functionality, any other expression for $f(\rho)$ can be considered in the numerical solution of eq 1. Thus, tabulated data from experiments or continuous time random walk simulations[14] carried out at a constant density of electrons can be used to define $f(\rho)$, which is subsequently inserted in eq 1. In this way, we conveniently separate a microscopic process (electron diffusion in a mesoporous semiconductor) from the macroscopic problem related to the solution of the diffusion−recombination equation for a working electrode with appropriate boundary conditions.

Results and Discussion

Short-Circuit Conditions. The continuity eq 1 can be solved under short-circuit conditions with the appropriate boundary conditions (eq 4). Hence we take the electron density at the working electrode and at zero time to be equal to the electron density in the dark, for which we used a value of 10^{22} m^{-3} (see ref 16). In addition, a value of 10^{-11} m^2 s^{-1} has been assumed[16] for the diffusion coefficient in the dark D_0. Nevertheless, the short-circuit currents obtained numerically are seen to be independent of the actual values used for ρ_0 and D_0. These parameters only affect time evolution of the current before the stationary state is reached. Note also that the dark value D_0 is implicitly affected by the total density of traps via eq 9. Thus more traps imply a lower diffusion coefficient (lower mobility). The total density of traps will again affect the time evolution of the current but not the steady-state value of the current.

We have used mesoporous TiO_2 cells sensitized with chlorophyll extracts (see Appendix A) as an experimental reference for our numerical results. These cells have short-circuit currents of around 0.20−0.25 mA cm^{-2} and open-circuit voltages of around 600−650 mV. To reproduce the experimental current for a realistic absorption spectrum of the dye, the quantum yield of injection is adjusted (see Appendix B for details). To test the numerical accuracy of the numerical model, we have carried out calculations without recombination ($k_{R,0} = 0$). Under these conditions, the ECCE should be ideally 1. The results are shown

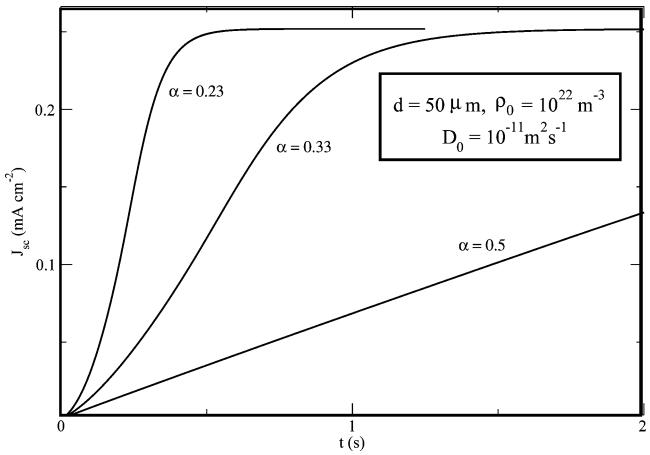

Figure 2. Short-circuit current density versus time for different values of the trap distribution parameter α. The results where obtained from the solution of the continuity equation using a DSSC sensitized with chlorophyll as the experimental reference.

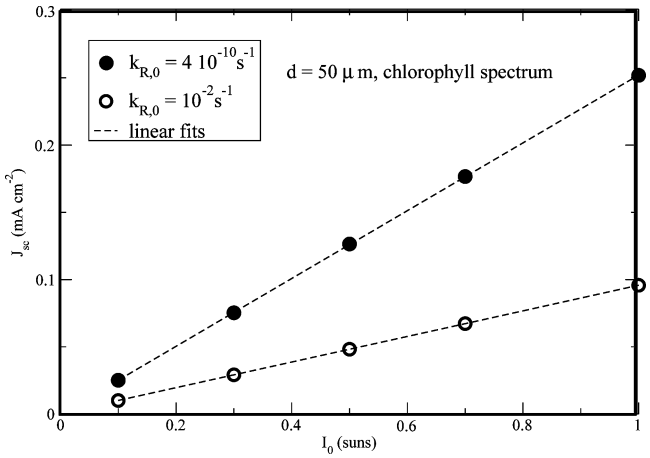

Figure 3. Steady-state short-circuit current density as a function of illumination intensity. Two values of the recombination constant where used. One was chosen to reproduce the experimental value of V_{oc} of a chlorophyll cell. The second was chosen ad hoc to show the effect of recombination on the current. In both cases the dependence of the current on the illumination intensity is linear.

in Table 1, showing values very close to 1. Ignoring recombination is a good approximation for the situation under short-circuit conditions. In this context, it is observed that the recombination constant that gives the correct open-circuit voltage provides, within numerical errors, the same short-circuit current as found for $k_{R,0} = 0$. We make use of this property to extract the quantum yield of injection for the actual cells prepared (see Appendix B).

Since the short-circuit collection efficiencies in the stationary state in the DSSCs are close to 1, no information about electron transport can be obtained from the short-circuit current. Nevertheless we can look at the time evolution of the current before the stationary limit is reached, which is defined by the rise time (time for the system to reach half the value of the stationary current). Results are presented in Table 1 and Figure 2. The results show that the system approaches the stationary state faster when α is small. This simply reflects the effect of having a diffusion coefficient that depends more strongly on electron density. According to this, films for which the relative proportion of deep traps is small present a faster response to illumination.

We have also determined the light-intensity dependence of the short-circuit current, and the results are shown in Figure 3. We obtain straight lines in all cases, even for a recombination constant that reduces the short-circuit current well below the experimental value (for which the ECCE departs substantially from 1). We can explain these results if we take into account that at short-circuit the following expression holds

$$J_{sc} = \Phi I = (\mathrm{ECCE} \times \mathrm{LHE} \times \phi_{inj}) I \qquad (14)$$

Since the LHE and the quantum yield of injection do not depend on illumination intensity, the light-intensity dependence of the current is controlled by the ECCE only. This in turn can be related to the effective diffusion length, l, given by

$$l = (D\tau)^{1/2} \qquad (15)$$

where D is the diffusion coefficient (eq 11) and τ is the lifetime of the electrons, which is related to the inverse of the recombination constant k_R in eq 13. According to the anomalous diffusion model utilized here, the effective diffusion coefficient should increase with electron density, which means that it gets larger at higher illumination intensity. However, the recombination rate should also increase with illumination intensity because a larger electron density enhances the probability of recombination of the electrons. Thus, diffusion and recombination have opposite effects when the number of incident photons is increased. Whether the collection efficiency varies or not depends on the relative variation of D and τ with electron density. If we consider that D and k_R $(1/\tau)$ vary with density according to eqs 11 and 13, then both quantities have exactly the same but opposite trends. Therefore, the diffusion length of eq 15 and, hence, the collection efficiency should not vary with light intensity, and the current is a linear function of light intensity. This compensation effect has been already pointed out by other authors.[19,20] Any departure from the linear functionality implies an extra enhancement of diffusion versus recombination or vice versa or the consideration of other effects such as intensity-dependent injection or hindered diffusion from the ions in the electrolyte.

Cells with an External Load. Cells with external resistive loads can be modeled if an appropriate functionality for the electron density at the working electrode is taken into account. In the presence of a voltage or at higher illumination intensity the electron density in the film should increase. To estimate this quantitatively we again apply the assumption that the distribution of trap energies is exponential-like (see eq 10). Using the Boltzmann approximation to the Fermi−Dirac distribution, we obtain that at zero temperature the total density of electrons corresponds to the integral of the distribution of traps between $-\infty$ and the quasi-Fermi level E_F[14]

$$E_F = -\frac{kT}{\alpha} \ln\left(\frac{\rho}{N_t}\right) \qquad (16)$$

From this expression we obtain for the electron density under illumination and in the dark

$$\rho = N_t \exp(-\alpha E_F/kT) \qquad (16a)$$

$$\rho_0 = N_t \exp(-\alpha E_F{}^0/kT) \qquad (16b)$$

respectively. Considering that $E_F{}^0$ is equal to the potentials of the redox couple and counter electrode in the dark and assuming that the counter electrode voltage does not significantly change as a function of voltage under illumination,[25] it is found that[4] $e(E_F - E_F{}^0) = -V$, and we obtain for the density of electrons

$$\rho(V) = \rho_0 \exp(\alpha eV/kT) \qquad (17)$$

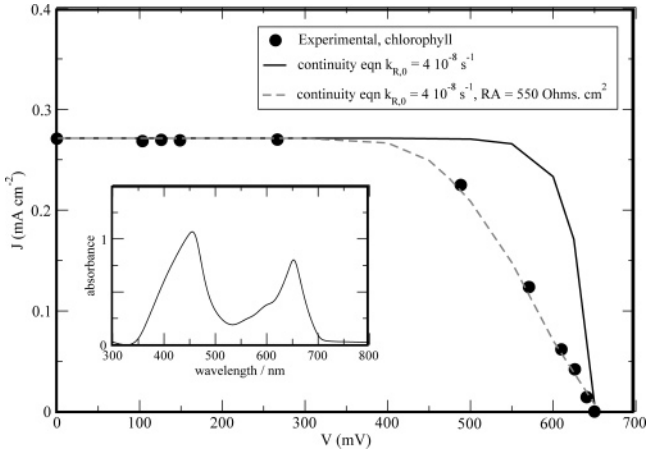

Figure 4. Illustration of the modeling of the current−voltage characteristics of a DSSC prepared in this work (d = 50 μm, A = 1 cm^2), corresponding to a cell sensitized with the extract of fresh green leaves whose UV−Vis spectrum is shown in the inset. The solid line corresponds to the current as obtained from the numerical solution of the continuity equation with no series resistance. The effect of the introduction of a series resistance is represented by the dashed line. All parameters shown correspond to the fitting of the model in order to reproduce the experimental short-circuit current and open-circuit voltage, i.e. $k_{R,0} = 4\ 10^{-8}\ s^{-1}$, $\phi_{inj} = 0.112$. See Appendix B for details.

This expression is consistent with the experimental measurements of Peter and co-workers,[26] where a linear relationship was found between the logarithm of the trapped electron density and the photovoltage. Also, capacitance measurements by Van de Lagemaat and co-workers[8] show similar results. This expression modifies the boundary condition in eq 4 for which the continuity equation is solved. Solving for different voltages we obtain the current−voltage curve. A typical result for this is shown in Figure 4.

The current−voltage curve obtained within the present model is a consequence of balance between external collection, controlled by the diffusion coefficient, and the back reaction, controlled by the recombination kinetic constant, both being dependent on electron density. At larger voltages, the overall electron density increases, and this enhances recombination and reduces the current. The open-circuit voltage V_{oc} is the voltage for which the current is found to be zero. Thus, by tuning the recombination constant $k_{R,0}$, we can fit the experimental open-circuit voltage. Through the use of this method, it is observed that V_{oc} happens to be independent of α.

It is interesting to see how the current−voltage characteristics arise from the numerical model employed here. In Figure 5 the electron density profiles in the stationary state at various values of the photovoltage are shown. It is observed that the density gradient that drives the electrons to the working electrode becomes smaller as the load to the cell is increased. At values of V close to open-circuit conditions, the density profile becomes virtually horizontal. We must bear in mind, however, that the current is determined by the product of the electron density gradient and a diffusion coefficient that depends strongly on the absolute electron density via eq 11.

The current−voltage curves obtained with the model used here can be fitted to the diode equation[27]

$$J = J_{sc} - J_0[\exp(eV/mkT) - 1] \qquad (18)$$

where J_0 is the exchange current density and m is the ideality factor. The numerical model defined by eqs 1, 4, 12, and 17 yields current−voltage characteristics with $m = 1$, corresponding to ideal behavior.

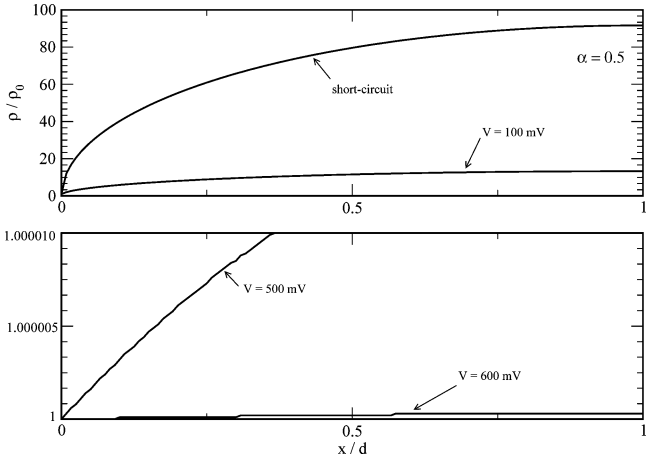

Figure 5. Electron density profiles for $\alpha = 0.5$ under the steady-state conditions as obtained from the solution of the continuity eq 1 for d = 50 μm, $\rho_0 = 10^{22}$ m^{-3} and $D_0 = 10^{-11}$ m^2 s^{-1}. Densities are shown in reduced units of $\rho(V)$ given by eq 17.

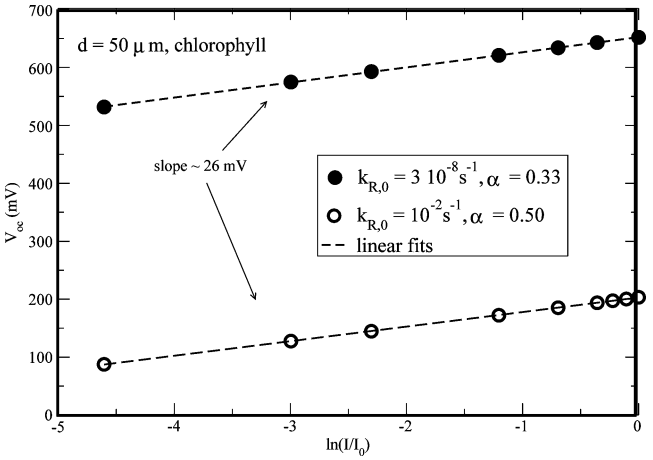

Figure 6. Light-intensity dependence of the open-circuit voltage as obtained from the numerical model. Results for two different recombination constants and two different values of the trap density parameter α are shown. In both cases the slope of the linear fits corresponds, within the numerical error, to an ideal diode (59 mV/decade).

Dependence of the Open-Circuit Voltage on Light Intensity and the Departure from Ideal Diode Behavior. The method devised in the previous section can be used to obtain the open-circuit voltage V_{oc} (V for which the current becomes zero). We can perform this calculation at various illumination intensities, extracting in this way the dependence of V_{oc} on light intensity. This will tell us what the implications are for our model of anomalous diffusion combined with trap-limited recombination. In Figure 6 we present semilogarithmic plots of the open-circuit voltage as a function of light intensity.

As mentioned above, the use of the model as defined by eqs 1, 4, 12, and 17 leads to ideal diode behavior. This is also shown in the slope of the V_{oc} curve versus the logarithm of illumination intensity, which amounts to $kT/e \approx 26$ mV (59 mV/decade), independent of the value of α. To explain the ideal diode behavior of our anomalous diffusion model, we use the following argument: At open-circuit conditions, recombination should equal generation. Thus, we can write

$$J_R(V_{oc}) = eG \qquad (19)$$

where J_R is the recombination current at the open-circuit voltage and G is the total generation term, which is proportional to the light intensity I. The recombination current can be related in

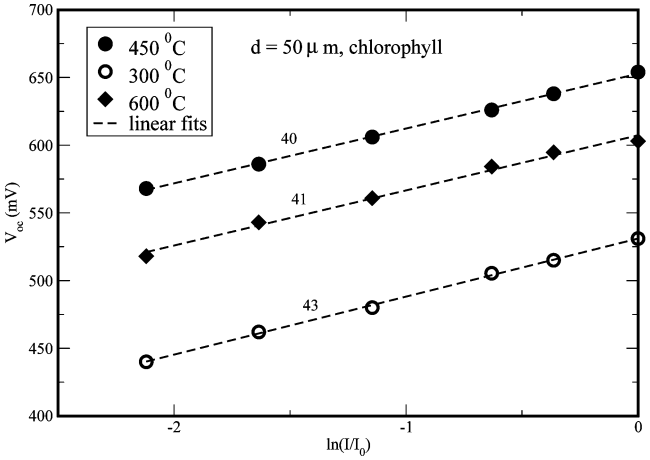

Figure 7. Light-intensity dependence of the open-circuit voltage as obtained experimentally with chlorophyll-sensitized DSSCs, with the TiO_2 films sintered at different temperatures. The slopes of the linear fits measured in millivolts are indicated in the graph.

turn to electron density. If we assume that $\rho \gg \rho_0$, then we can write the recombination current in the form (see eq 13)

$$J_R(V_{oc}) = ek_R(\rho - \rho_0) = ek_R\rho = ek_{R,0}f(\rho)\rho \qquad (20)$$

Combining eqs 12, 19, and 20, we find the following relationship between electron density and light intensity

$$\rho(V_{oc}) \propto I^{\alpha} \qquad (21)$$

This nonlinear dependence of the electron density on the light intensity has been observed experimentally with exponents that range between 0.45 and 0.6.[28,29] If we now consider simultaneously the functionalities contained in eq 17 at $V = V_{oc}$ and eq 21, then we find that the density dependence included in the parameter α cancels out in both equations. Hence we come to the following expression for the open-circuit voltage

$$V_{oc} \propto \frac{kT}{e} \ln I \qquad (22)$$

which corresponds to a linear function with a slope of 26 mV (ideal diode behavior) and *independent* of α. This is what is also observed in the numerical application of our model (Figure 6). To shed some light on this issue, we have performed experiments with DSSCs in which we have used the sintering temperature of the mesoporous oxide (Appendix A) as a simple parameter to modify the quality of the film, which would be expected to change the value of α. Results are shown in Figure 7; although the slope of V_{oc} versus the logarithm of the intensity obtained is not 26 mV, the slope remains approximately constant for different qualities of the TiO_2 film. According to these considerations, a change in the trap density or distribution through the parameter α, which is related to the material and the morphology of the mesoporous, nanostructured film, will not modify either the open-circuit photovoltage of the solar cell or its light-intensity dependence. Bearing in mind that a similar conclusion was drawn from the results under short-circuit conditions, improving the photoconducting properties of the film by decreasing the density of trap states or reducing the relative proportion of deep traps would not result in a better performance of the cell. This general conclusion has previously been mentioned by several authors based on a variety of experiments.[4,19] Note that these results are valid when the recombination kinetics are dominated by the electron transport kinetics inside the nanostructured film.

The observation that improving the photoconductivity does not increases cell performance is especially evident when we evaluate the full current−voltage curve, from which the efficiency of the cell can be extracted. The compensation effect that makes current and voltage independent of α holds for the entire current−voltage curve according to the numerical model employed here. Hence for a cell with virtually zero series resistance the electrical output would reach a maximum and the fill factor would be very close to 1. A finite series resistance can easily be introduced in the present model (Appendix B). Although this can help to fit experimental current−voltage curves with lower fill factors (Figure 4), the inclusion of the series resistance does not modify the intensity dependence of the open-circuit voltage. In the literature, several examples of ideal diode behavior have been reported where the slope of the V_{oc} versus log(I) is 26 mV[30−32] for relatively large irradiances. However, others have reported larger slopes between 37 and 53 mV,[33,34] indicating that the dependence of the open-circuit voltage on light intensity may be more complex. The explanation has to be sought in a different dependence of the recombination rate constant on the electron density, for example, by including the transfer of electrons to the electron acceptor as a rate-determining step. The relative importance of the anomalous transport kinetics in the nanostructured film and the kinetics of transfer to the electron acceptor is expected to depend on the electron density. In addition, this may depend on specific experimental conditions.

Conclusions

In this work we have implemented a numerical model based on the solution of the continuity equation with density-dependent diffusion and recombination terms. We have calculated the current−voltage curve and determined the dependence of the short-circuit current and the open-circuit voltage on the light intensity within the assumptions of the model. For the case where recombination is assumed to be determined by the electron transport kinetics in the nanostructured film, the numerical results lead to ideal diode behavior. This is shown to be a consequence of a compensation effect related to the opposite trends by which the diffusion coefficient and the electron lifetime vary with electron density.

As a consequence, the light-intensity dependence of the short-circuit current and open-circuit voltage are not dependent on the parameter α that describes the trap state distribution function, which determines the electron transport properties. Hence, changing the trap state distribution by changing the material or morphology of the nanostructured film will not have a significant effect on cell performance, at least under steady-state conditions, since improving the conducting properties of the nanostructured oxide electrodes also results in faster recombination. Under these circumstances, efforts to improve DSSC photoconversion efficiencies should be devoted to deactivate recombination by modifying the interface parameters rather than by improving the electron collection.

Acknowledgment. J. A. Anta and F. Casanueva thank the Ministerio de Educación y Ciencia of Spain for funding under grant ENE2004 01657 and the Universidad Pablo de Olavide for support from the program "Plan Propio de Investigación". G. Oskam thanks the Consejo Nacional de Ciencia y Tecnología (CONACYT) of Mexico for funding under project number 43828-Y. We also thank Degussa Spain S. A. and DuPont Spain for providing chemicals and materials for research.

Appendix A: Experimental Procedures

Experiments were carried out using dye-sensitized TiO_2 mesoporous films in a thin layer solar cell. The TiO_2 film was prepared using procedures described in the literature[35,36] from commercial colloidal TiO_2 powder (Degussa P-25) with an average nanoparticle size of about 20 nm.

The TiO_2 powder and 20 mL of nitric acid solution (pH 3−4) were mixed together until a viscous suspension with a concentration of 350 g/L was obtained. The suspension was spread onto the transparent electrode with a glass rod, using tape for controlling the film thickness, and was allowed to dry in air. The tape was removed, and the film was heated to 450 °C for 30 min. Other temperatures were also employed (Figure 7). The sensitizing solution consisted of a chlorophyll extract from fresh leaves of an orange tree. The leaves were crushed with acetone until a dark green solution was obtained. To sensitize the TiO_2, the electrode was immersed in the chlorophyll solution for 24 h. The counter electrode was prepared by spreading a drop of hexachloroplatinic acid (0.01 M in 2-propanol) on the conductive side of another transparent electrode and then annealing at 380 °C for 10 min. The electrolyte solution was prepared by dissolving 2.0 g of KI and 0.3 g of I_2 in 25 mL of propylene carbonate (HPLC grade). Permanent sealing was accomplished by binding together the two electrodes with DuPont Surlyn 1702.

UV−vis absorption spectra were recorded on an Ocean Optics high-resolution spectrometer. Short-circuit current and open-circuit voltage measurements were obtained using a TTI 1750 multimeter while the cell was illuminated by a Thermo Oriel Xenon arc lamp, equipped with an IR−UV blocking filter. Current−voltage curves were measured by a series of resistances as the variable load. The light intensity was adjusted by means of a combination of neutral density filters for irradiances ranging from 0.1 to 1 sun.

Appendix B: Modeling Real Dye-Sensitized Solar Cells

To quantitatively describe the electrical output of the DSSCs prepared in this work using the numerical model presented, we operated according to the following steps:

(1) We estimate the light absorption spectrum of the dye adsorbed onto the TiO_2 from the absorption spectrum in solution (see inset in Figure 4). To do this we use

$$\alpha_{ab}(\lambda, \text{cell}) = \alpha_{ab}(\lambda, \text{solution}) \times \frac{C_{dye}(\text{cell})}{C_{dye}(\text{solution})} \qquad \text{(A-1)}$$

where C_{dye} stands for the molar concentrations of the dye in the solution and in the cell. The former is estimated from the measured absorbance at the maximum and the tabulated extinction coefficient of the dye at the same wavelength. The latter is derived from the estimated internal surface of the TiO_2 electrode assuming a roughness factor of 1000 and a mean area of 1 nm^2 per dye molecule.

(2) We adjust the quantum injection yield ϕ_{inj} in eq 2 by fitting the experimental current under short-circuit conditions. In these calculations the recombination rate is assumed to be zero by taking $k_{R,0} = 0$. Values for ϕ_{inj} between 0.07 and 0.1 are found for chlorophyll cells.

(3) Once ϕ_{inj} is fixed, the recombination constant $k_{R,0}$ is adjusted by making the current zero at the experimental open-circuit voltage V_{oc}.

(4) The current−voltage curve is obtained by solving at different voltages from 0 to V_{oc}.

(5) The light-intensity dependence is obtained by repeating the above procedure at a different illumination intensity. This is achieved by varying the factor F in eq 3.

(6) If a series resistance is required, then we follow an iterative procedure. The voltage V entering eq 18 is replaced by $V = V + JAR$, where J is the current, A the cell surface, and R the resistance. The equation is solved for this new voltage, and the new current obtained is utilized to modify the voltage. The process is repeated until the current yielded by the numerical model does not vary. In this way we have obtained the results shown in Figure 4 for the values shown.

References and Notes

(1) O'Regan, B.; Grätzel, M. *Nature* **1991**, *353*, 737.

(2) Grätzel, M. *J. Photochem. Photobiol., A* **2004**, *164*, 3.

(3) Hagfeldt, A.; Grätzel, M. *Chem. Rev.* **1995**, *95*, 49.

(4) Frank, A. J.; Kopidakis, N.; Van de Lagemaat, J. *Coord. Chem. Rev.* **2004**, *248*, 1165.

(5) Nelson, J.; Chandler, R. E. *Coord. Chem. Rev.* **2004**, *248*, 1181.

(6) Bisquert, J.; García-Belmonte, G.; Fabregat Santiago, F. *J. Solid State Electrochem.* **1999**, *3*, 337.

(7) Van de Lagemaat, J.; Frank, A. J. *J. Phys. Chem. B* **2001**, *105*, 11194.

(8) Van de Lagemaat, J.; Park, N. G.; Frank, A. J. *J. Phys. Chem. B* **2000**, *104*, 2044.

(9) Schwarzburg, K.; Willig, F. *Appl. Phys. Lett.* **1991**, *58*, 2520.

(10) De Jongh, P. E.; Vanmaekelbergh, D. *Phys. Rev. Lett.* **1996**, *77*, 3427.

(11) Könenkamp, R. *Phys. Rev. B* **2000**, *61*, 11057.

(12) Bisquert, J.; Zaban, A. *Appl. Phys. A* **2003**, *77*, 507.

(13) Nelson, J. *Phys. Rev. B* **1999**, *59*, 15374.

(14) Anta, J. A.; Nelson, J.; Quirke, N. *Phys. Rev. B* **2002**, *65*, 125324.

(15) Scher, H.; Montroll, E. *Phys. Rev. B* **1975**, *12*, 2455.

(16) Cao, F.; Oskam, G.; Meyer, G. J.; Searson, P. C. *J. Phys. Chem.* **1996**, *100*, 17021.

(17) Fisher, A. C.; Peter, L. M.; Ponomarev, E. A.; Walker, A. B.; Wijayantha, K. G. U. *J. Phys. Chem. B* **2000**, ***104***, 949.

(18) Nelson, J.; Haque, S. A.; Klug, D. R.; Durrant, J. R. *Phys. Rev. B* **2001**, *63*, 205321.

(19) Kopidakis, N.; Benkstein, K. D.; Van de Lagemaat, J.; Frank, A. J. *J. Phys. Chem. B* **2003**, *107*, 11307.

(20) Bisquert, J.; Vikhrenko, V. S. *J. Phys. Chem. B* **2004**, *108*, 2313.

(21) In the present state of development the model only considers electron diffusion. Ion transport in the electrolyte can be included as well.

(22) Press, W. H. *Numerical Recipes in C: The Art of Scientific Computing*; Cambridge University Press: New York, 1992.

(23) Schwarzburg, K.; Ernstorfer, R.; Felber, S.; Willig, F. *Coord. Chem. Rev.* **2004**, *248*, 1259.

(24) Haque, S. A.; Tachibana, Y.; Klug, D. R.; Durrant, J. R. *J. Phys. Chem. B* **1998**, *102*, 1745.

(25) Oskam, G.; Bergeron, B. V.; Meyer, G. J.; Searson, P. C. *J. Phys. Chem. B* **2001**, *105*, 6867.

(26) Peter, L. M.; Duffy, W.; Wang, R. L.; Wijayantha, K. G. U. *J. Electroanal. Chem.* **2002**, *127*, 524.

(27) Nelson, J. *The Physics of Solar Cells*; Imperial College Press: London, 2003.

(28) Franco, G.; Gehring, J.; Peter, L. M.; Ponomarev, E. A.; Uhlendorf, I. *J. Phys. Chem. B* **1999**, *103*, 692.

(29) Schlichthörl, G.; Park, N. G.; Frank, A. J. *J. Phys. Chem. B* **1999**, *103*, 782.

(30) Bergeron, B. V.; Marton, A.; Oskam, G.; Meyer, G. J. *J. Phys. Chem. B* **2005**, *109*, 973.

(31) Liu, Y.; Hagfeldt, A.; Xiao, X.-R.; Lindquist, S.-E. *Sol. Energy Mater. Sol. Cells* **1998**, *55*, 267.

(32) Salvador, P.; Gonzalez-Hidalgo, M.; Zaban, A.; Bisquert, J. *J. Phys. Chem. B* **2005**, *109*, 15915.

(33) Schlichthörl, G.; Huang, S. Y.; Sprague, J.; Frank, A. J. *J. Phys. Chem. B* **1997**, *101*, 8141.

(34) Cameron, P. J.; Peter, L. M.; Hore, S. *J. Phys. Chem. B* **2005**, *109*, 930.

(35) Cherepy, N. J.; Smestad, G. P.; Grätzel, M.; Zhang, J. Z. *J. Phys. Chem. B* **1997**, *101*, 9342.

(36) Graziani, C. G.; Polo, A. D.; Iha, N. Y. M. *J. Photochem. Photobiol., A* **2003**, *160*, 87.